NOVEL AND VERSATILE TiO_2 THIN FILMS ON PET FOR PHOTOCATALYTIC REMOVAL OF CONTAMINANTS OF EMERGING CONCERN FROM WATER

Rafaela B. P. Marcelino[1], Camila C. Amorim[1*], Marina Ratova[2], Brice Delfour-Peyrethon[2], Peter Kelly[2]

[(1)] Universidade Federal de Minas Gerais, School of Engineering, Department of Environmental and Sanitation Engineering, Research Group on Environmental Applications of Advanced Oxidation Processes, Av. Antônio Carlos, 6627, Belo Horizonte – MG, Brazil.

[(2)] Manchester Metropolitan University, Faculty of Science and Engineering, Surface Engineering Group, Manchester, M1 5GD, U.K.

[*] E-mail: <camila@desa.ufmg.br> Telephone: +55 3134093677

Abstract

The current work presents new and versatile photocatalytic surfaces designed to remove contaminants of emerging concerns (CECs) from water. Photocatalytic thin films of titanium dioxide (TiO_2) were deposited on a polyethylene terephthalate (PET) surface (PET- TiO_2) and photosensitized by a natural and non-hazardous curcumin (turmeric). The nanocrystalline TiO_2 thin film was deposited in a single stage and solvent-free process, without thermal post treatment, using the high power impulse magnetron sputtering (HiPIMS) technique. The photocatalytic film was characterized by different techniques (SEM/EDS, STEM, AFM, UV-Vis spectroscopy, and wettability via water droplet contact angle measurements). The photocatalytic activity was assessed by the degradation of two model CECs: the fungicide carbendazim (CBZ), used in different crops around the world (coffee, rice, fruits, etc.), and the anthropogenic pollution tracer caffeine (CAF). Removal of these model CECs of up to 39% were achieved under

combined UV and visible irradiation under 7 h photocatalytic treatments. The degradation process was further studied by organic carbon dissolved analysis, with 80% removal achieved, and acute ecotoxicity tests with *Aliivibrio fischeri* bacteria, indicating reduction of toxicity or non-change. The PET-TiO_2 surfaces remained stable for 5 consecutive cycles of use, with similar kinetic rates. Finally, the species involved in photocatalytic reactions were investigated by use of h^+, $HO^\bullet$ and $^\bullet O_2^-$ trapping agents for the degradation reactions, both in the presence and absence of turmeric. The results were indicative of the fact that the addition of the turmeric led to an increase in photogenerated $^\bullet O_2^-$ radicals due to a synergistic effect between the photocatalyst and photosensitizer. The results demonstrate the potential of the PET-TiO_2 surfaces as a straightforward solution for the removal of CECs in wastewater treatment plants (WWTP), using a flexible, scalable, reusable and environmental friendly photocatalytic material.

Keywords: Advanced oxidation processes; contaminants of emerging concern; polyethylene terephthalate (PET); high power impulse magnetron sputtering; surface engineering; photosensitization.

1. Introduction

Photocatalysis has become of great environmental interest in the last century, since the discovery of the photoactivity of titanium dioxide (TiO_2) crystalline polymorphs. It has proved to be useful as a tertiary treatment technology, which can couple both disinfection and removal of biorecalcitrant compounds, such as contaminants of emerging concern (CEC) [1]. CECs have been detected in different environmental sectors [2], at concentrations varying between some ng L^{-1} and several μg L^{-1}. Owing to the development and dissemination of analytical techniques, the world has become aware of the occurrence of CECs [3]. This awareness combined with the fact that the removal rates of CECs in urban wastewater treatment plants (WWTP) are rather low,

evidence the need for improvements in treatment techniques in order to achieve enhanced water quality and provide a safe aquatic environment.

In order to remove CECs from water matrices, different photocatalytic processes have been extensively studied in the last decades [4], such as the classical UV-A/TiO_2 for the degradation of antibiotics [5–7], agrochemicals [8,9] carbamazepine (antiepileptic/ analgesic) [6,7,10], caffeine [6], bisphenol A [11,12] and hormones [13,14]. However, the use of a photocatalyst in its powdered form poses some difficulties in the catalyst recovery and reuse. Many attempts have been made to support the photocatalyst in different matrices [15,16] and surface engineering is playing an important role by providing different techniques, including magnetron sputtering, for the production of photocatalytic thin films.

Magnetron sputtering is a widely used commercial deposition technique for many functional films, including photocatalytic coatings [17,18]. Due to elevated process temperatures (>250 °C) and/or the requirement for post-deposition annealing, conventional magnetron sputtering may not be able to deposit anatase titania onto polymeric supports [19].

However, high power impulse magnetron sputtering (HiPIMS), a relatively recently introduced variant of the process, has proven able to deposit photocatalytically active titania coatings directly onto flexible polymeric substrates in a single stage process. [20,21]. Furthermore, HiPIMS is a scalable technique which is actively being developed for industrial scale production by several companies in applications ranging from tool coatings to roll-to-roll systems for depositing functional films onto polymeric web of a

wide range of thicknesses. Thus, the process has the potential for large scale production of coated web materials of different grades to suit multiple applications.

Organic polymers have potentially wide applicability as flexible substrates for the deposition of photocatalytic films [19,22], given the ease in which they can be formed into shapes post-deposition. PET (Polyethylene terephthalate) is recyclable and it is considered one of the most important engineering plastics owing to its excellent tensile and impact strength, chemical resistance, clarity, processability, colourability and reasonable thermal stability [23,24]. Moreover, the TiO_2 thin films deposited onto PET substrates might work as a UV-protective layer, since they absorb UV light, increasing the life time of the polymeric material [25,26].

Photosensitization is a reaction to radiation that is mediated by a light-absorbing molecule (photosensitizer - PS), which is not the ultimate target. There are different types of PS, and coloured compounds such as dyes have been used in dye-sensitized solar cells [27–29], photodynamic therapy [30,31] and dye-sensitized photocatalysis in order to extend the photo-response of the semiconductor into the visible region [32,33]. Thus, the efficiency of the photocatalyst can be improved by the use of PS, since it can enhance the visible-light harvesting and promote charge transfer between the PS and TiO_2, and this is important since TiO_2 is generally non-responsive to visible light [34,35]. Ag_2S [35], eosin Y [36], methylene blue [37], alizarin red S [33], erythrosin B [38] and rhodamine B [37] are some examples of PS that have been used. In this work the non-toxic turmeric, a natural source of curcumin [39,40], was selected to be used in order to mediate the photocatalytic degradation of two CEC model pollutants, caffeine (CAF) and carbendazim (CBZ) .

The efficiency of the photocatalyst can be improved by the use of PS since it can enhance the visible-light harvesting and promote charge transfer between the PS and TiO_2, and this is important since TiO_2 is generally non-responsive to visible light [34,35]. In this work the non-toxic turmeric, a natural source of curcumin [39,40], was selected to be used in order to mediate the photocatalytic degradation of two CEC model pollutants, caffeine (CAF) and carbendazim (CBZ) .

CBZ is a systemic benzimidazole fungicide highly consumed worldwide [41], and was selected since it is potentially an endocrine disruptor [42], classified as "priority hazard substance" by the Water Framework Directive of the European Commission [9], and as Group C - Possible Human Carcinogen by USEPA, 2006 [43]. Under natural environmental conditions, it is very stable and it has been frequently detected in different water matrices [44,45].

CAF is a natural alkaloid produced by many plant species and is the most widely used central nervous system stimulant [46]. Although the human body is efficient at metabolizing it, between 0.5 – 10% is excreted unchanged, mostly in urine [47]. Moreover, the molecule has been demonstrated to be chemically and photochemically stable, therefore its content may not be significantly reduced through traditional WWTP. In this way, CAF has been detected worldwide in surface water and wastewater [47,48], groundwater [49], marine water [50] and drinking water [51]. Consequently, it has been used as an indicator of anthropogenic pollution [47,48,50].

In this context, this work presents the performance of new photocatalytic surfaces made with thin films of TiO_2 deposited on flexible PET sheets via HiPIMS, photosensitized

by a natural curcumin source (turmeric), free of hazardous chemicals and a potential straightforward solution for the degradation of CECs from water sources.

2. Material and Methods

2.1 Coating deposition process and characterization of photocatalytic surface

TiO_2 thin films were deposited onto PET sheets (PET-TiO_2) by reactive magnetron sputtering in the HiPIMS mode in a single stage process from a 99.5% pure Ti target (300 mm x 100 mm) in an argon/oxygen atmosphere (3.0 sccm O_2 and 50 sccm Ar) at a pressure of 0.4 Pa. The oxygen flow rate was controlled by optical emission monitoring to provide stoichiometric TiO_2 coatings. The HiPIMS power supply (Huettinger HMP1/1_P2) was operated at 700 Hz pulse frequency with a 50 μs duration pulse and the voltage was set to 540 V. This resulted in a time averaged power of approximately 1.5 kW.

The coatings were deposited onto 1m long by 10 cm wide strips of 100 μm thick food-grade PET sheets, which were ultrasonically pre-cleaned in propanol prior to deposition. The substrates were mounted on a rotating drum substrate holder (1 m circumference) that was electrically floating. The deposition time was 1 h for all the samples.

An Ocean Optics USB4000 spectrometer was used for the UV-Vis transmittance measurements with subsequent calculation of the optical band gap values of the coatings made using the Tauc plot method [52], where the optical band-gap energy value (Eg) can be obtained using the absorption coefficient α (Eq. 1):

$$\alpha h\nu = \left(h\nu - E_g\right)^{\frac{1}{n}} \quad (1)$$

where α is the absorbance coefficient, h is the Plank constant, ν is the frequency of vibration, Eg is the energy band-gap and n is the exponent that denotes the nature of sample transition. For the indirect allowed transition, as in the case of titanium dioxide, n = 2.

The measurements of photoinduced wettability were performed via water droplet contact angles (ϕ) measured at the surface of the films using a contact angle goniometer (model Digidrop DI, France) at 25 ± 2 °C. Ten microliters of water were gently dropped on the surface of the material using a microsyringe. Samples were kept in the dark for 24 h prior to the contact angle measurements and irradiated with UV-A lamps (4 x 9 W bulbs with λ_{max} = 370 nm) for two hours before each measurement. All of the droplets were released from 1 cm above the surface to minimize any inconsistencies. The angle between the tangent line and the coating surface from the goniometric scale was measured 30 s after the release of each droplet onto the surface. Three consecutive measurements were performed, using the Surface Energy mode of the software, which enables a direct measurement of the contact angle (in degrees).

Scanning electron microscopy (SEM) analysis, coupled with energy-dispersive X-ray spectroscopy (EDS), were performed using both a JEOL JSM - 6360LV with an EDS detector at 15 kV and a Quanta FEG 3D FEI at 10 kV. Samples were mounted and coated with carbon prior to the SEM analysis. The coating cross-section morphology and thickness were evaluated through scanning transmission electron microscopy (STEM) analysis using a Tecnai G2-20 - SuperTwin FEI - 200 kV STEM microscope. Ultra-thin cross-sections of the samples for transmission analysis were prepared by ultramicrotomy, embedding and screen mounting.

Elementary composition and chemical state of the samples was investigated via STEM coupled with Electron Energy-Loss Spectroscopy (EELS). EELS analysis were performed with a Tecnai G2-20 - SuperTwin FEI - 200 kV transmission electron microscope coupled with EELS detector. The obtained EELS spectra were compared with a TiO_2 standard provided by The EELS Data Base (available at https://eelsdb.eu/).

Superficial morphology and roughness were evaluated through atomic force microscopy (AFM) with Cypher ES (Asylum Research) equipment with a scanning area of 900μm^2. The surface roughness was quantified by the root-mean-squared roughness (R_{rms}). R_{rms} is given by the standard deviation of the data from AFM topography micrographs, and determined using equation 1 [53]:

$$R_{rms} = \sqrt{\frac{\sum_{n=1}^{N}(z_n - \bar{z})^2}{N-1}} \quad (1)$$

where z_n represents the height of the nth data, $\bar{z}$ is the mean height of z_n in AFM topography and N is the number of the data analyzed. Each sample was analyzed in four different locations and R_{rms} results are the mean of these four different results for each sample.

All the experiments and analyses involving microscopy (SEM/EDS and STEM) and AFM were performed in the Centre of Microscopy at the *Universidade Federal de Minas Gerais*, Belo Horizonte, MG, Brazil (http://www.microscopia.ufmg.br).

2.2. Photocatalytic activity assessment

Analytical standard CBZ and CAF from Sigma-Aldrich were used to prepare a 15.6 μM solution with ultrapure water. A food grade (Kitano, Brazil) and non-toxic turmeric

(*Curcuma longa*), which is a source of curcumin, was used as a photosensitizer (PS). The PS was employed at a final concentration of 50 $mg.L^{-1}$ due to its solubility limit and it was previously dissolved in ethanol (1% m/v). The main physical-chemical properties are summarized in Table S1 (supplementary material). The PS was added to the aqueous solution at the beginning of each experiment and it was degraded by the end of the assessment.

The photocatalytic activity of the PET-TiO_2 was separately assessed for the degradation of 100 mL aqueous solutions of two model pollutants: CBZ or CAF, in the presence of turmeric (50 $mg{\cdot}L^{-1}$with 1% ethanol), using a UV-A/Vis photoreactor for 7 h. The photoreactor (Fig. 1-a) was equipped with four 9 W UV-A bulbs (λ_{max} = 370 nm) that were positioned above of the reaction vessel (Petri Plate, D = 9 cm, H = 3 cm, water depth ~ 2 cm), and housed in a 9 x 22 x 24 lamp support (Fig. 1-b). The emission spectrum of the lamp was measured with a USB2000+ XR1-ES (Ocean Optics) spectrometer (Figure 1-c). Temperature and pH were monitored at each sampling; the temperature was found to be 22 ± 2 ºC and pH = 7 ± 1 for all tests.

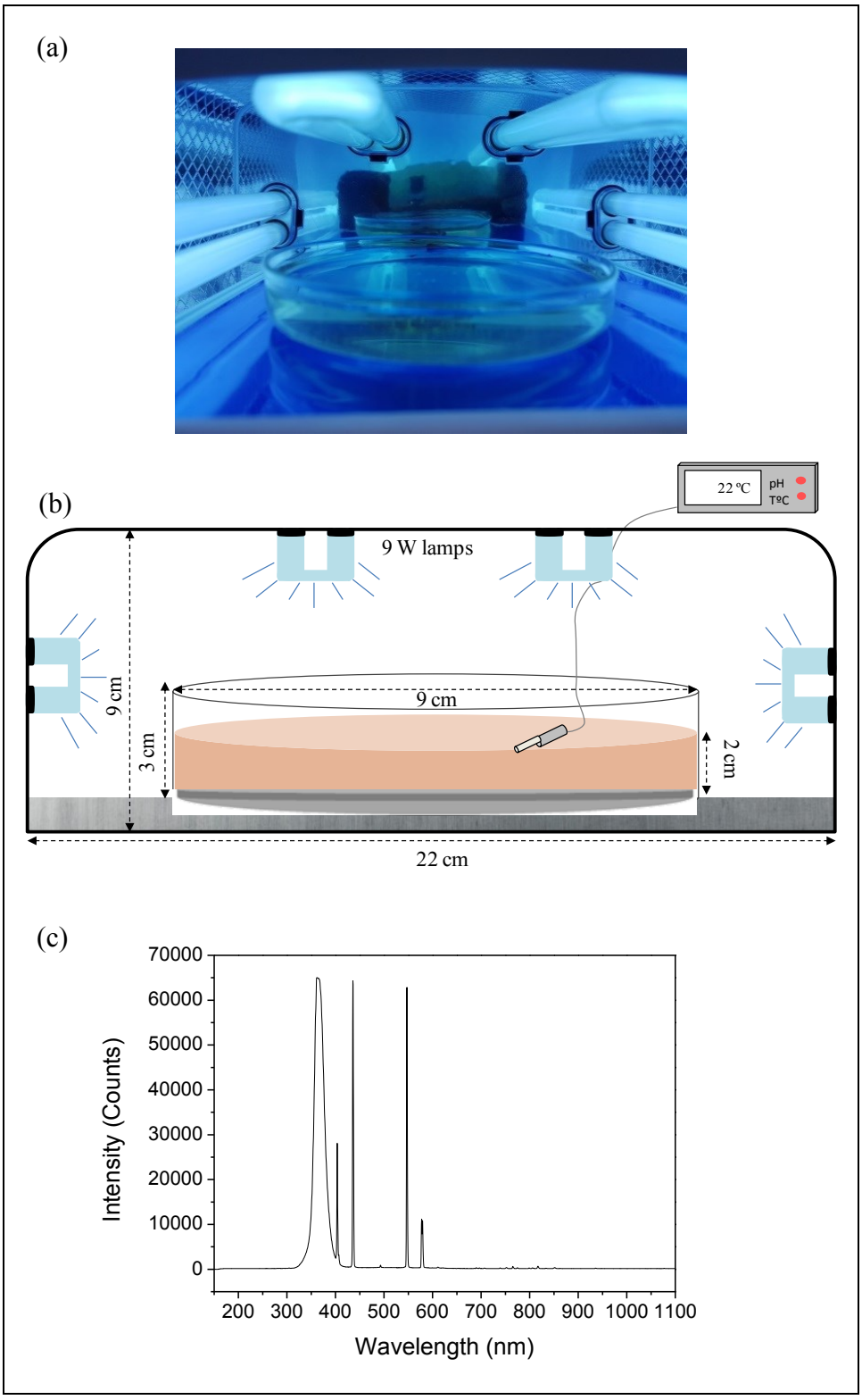

Fig. 1 – (a) The interior of the UV-A/Vis photocatalytic reactor, (b) a schematic representation of the reactor with its main dimensions and (c) the corresponding lamps emission spectrum.

The photocatalytic degradation of the CECs was investigated by UV-Vis spectrophotometry (Micronal AJX-3000PC spectrophotometer from 200-900 nm). Adsorption experiments (in the dark) followed by turmeric-mediated photolysis were performed in order to investigate the influence of curcumin and UV-A/Vis radiation on the removal of the CECs. Afterwards, photocatalytic experiments were performed in the same conditions with the presence of the new PET-TiO_2 photocatalytic surfaces. Organic matter mineralization was monitored through Dissolved Organic Carbon (DOC) analysis using TOC-V CPN equipment (Shimadzu).

The stability and reusability of the PET-TiO_2 samples were studied with 5 consecutive photocatalytic runs with CBZ. After each cycle, the film was washed thoroughly with deionized water, and a fresh solution of CBZ was added before the next photocatalytic run. Samples were submitted to atomic absorption spectrometry – AAS (VARIAN AA240FS), in order to assess TiO_2 leaching.

The toxicity of possible by-products formed during the photocatalytic reaction was investigated by acute ecotoxicity tests, which were conducted using the luminescent marine bacteria *Aliivibrio fischeri* (Microtox®) according to the methodology presented by Starling *et al.* (2017) [54]. Toxicity results were analysed using the EC_{50} (concentration that has an effect on 50% of the population under 30 minutes of exposure) and acute toxicity unit (a.T.U. = $100/EC_{50}$) values. The higher the a.T.U., the higher the toxicity.

2.3 Study of photogenerated species via trapping reactions

The photogenerated species involved in the photocatalytic reaction were studied employing 1 mM solutions of the following trapping agents: ethylenediaminetetraacetic

acid (EDTA) for h^+ [55,56], dimethyl sulfoxide (DMSO) for $HO^{\bullet}$ [57,58], and benzoquinone (BQ) for $^{\bullet}O_2^-$[57]. DMSO, EDTA and BQ scavengers were added individually to the CAF solution and submitted to a photocatalytic (with and without turmeric) run with the PET-TiO_2 surface in the same conditions of the previous experiments.

3. Results and Discussion

3.1 Coatings overview and characterization

The PET-TiO_2 surfaces were characterized before and after the photocatalytic activity tests in order to evaluate their reusability. Fig. 2 shows SEM micrographs of the surfaces of the uncoated PET substrate (Fig. 2a), the as-deposited PET-TiO_2 (Fig. 2b) and for the five times used PET-TiO_2 (Fig. 2c). In Fig. 2b, the highlighted area indicates where the EDS measurements were performed in detail.

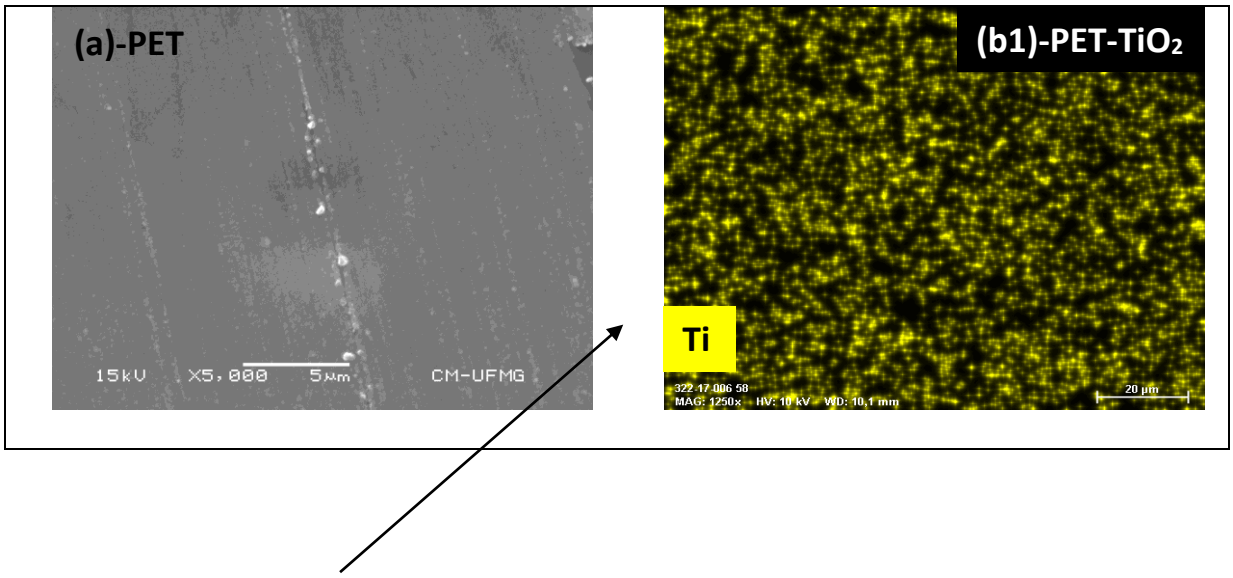

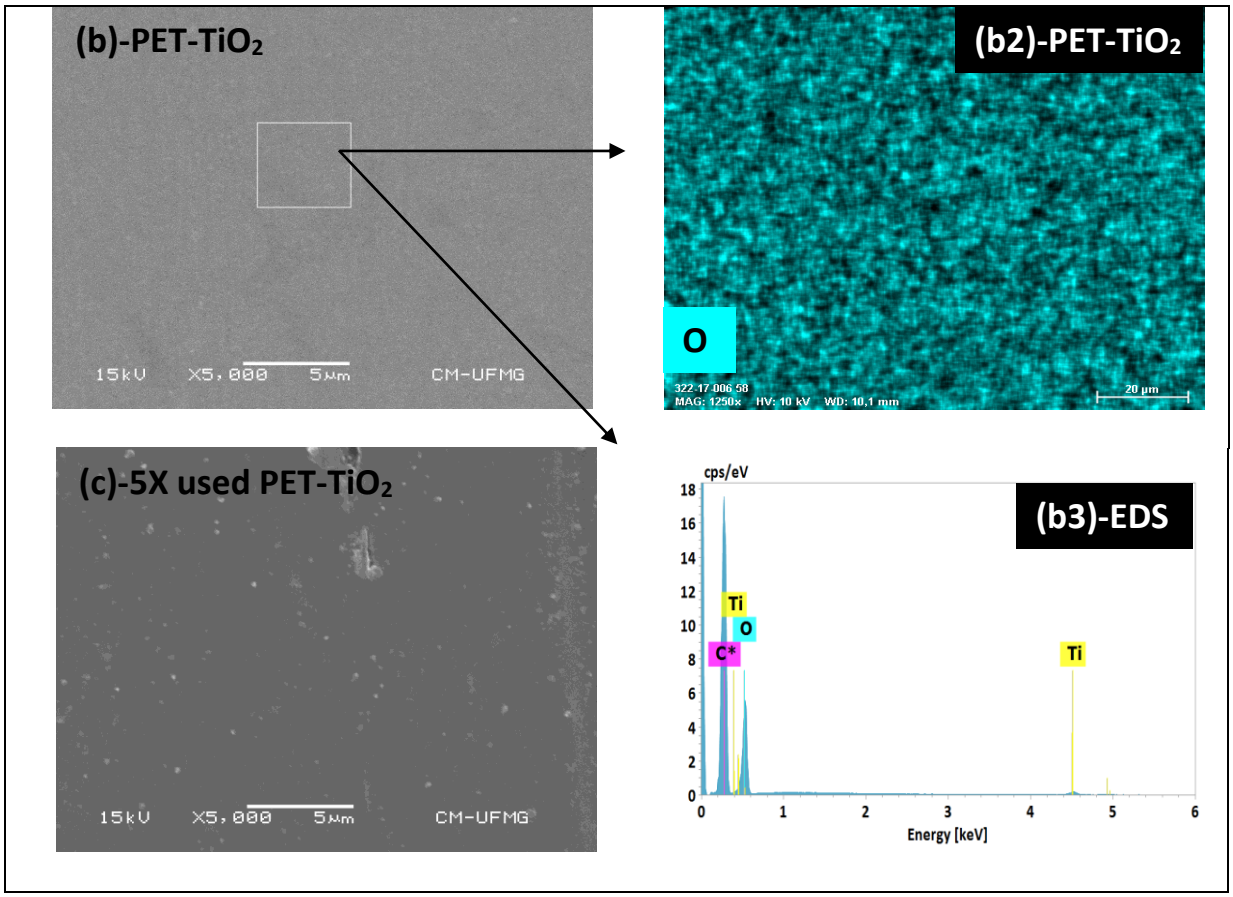

Fig. 2- SEM micrographs of: (a) uncoated PET substrate, (b) new PET-TiO_2 surface (c) 5x used PET-TiO_2 surface. SEM chemical mapping micrographs of the new PET-TiO_2 surface: (b1) titanium mapping, (b2) oxygen mapping, with corresponding EDS spectrum.

According to Fig. 2, the photocatalytic surfaces presented homogeneous, conformal and dense surfaces with the presence of some defects, which are assumed to be scratches on the PET substrate– Fig. 2(a) - and dirt and dust particles - Fig. 2(c) - that were in contact with the surfaces. A dense microstructure and smooth surface was expected, as different authors have reported such characteristics for TiO_2 coatings deposited by HiPIMS [22,59–61]. Indeed, other reported work, where TiO_2 films were deposited from a ceramic $TiO_{1.8}$ target found that HiPIMS-grown films exhibit significantly smoother

and denser surfaces than the coatings deposited by pulsed (DC) magnetron sputtering [60]. The same effect was observed for TiO_2 films grown from a metallic Ti target, as reported by [59].

Chemical mapping and EDS of the new PET-TiO_2 (Fig. 2 - b1, b2, b3) prove the predominance of carbon (PET and coating for SEM/EDS), titanium and oxygen elements. It can be seen that titanium is homogeneously distributed on the surface, and that it was detected from Kα (4.51 eV) and Lα (0.45 eV) characteristic peaks, (Fig. 1 - b3).

SEM results shown in Fig. 2 and EDS results (Table S2 – supplementary material) indicate that both used and new titania coated surfaces - Fig. 2(b) and 2(c) – presented similar surface morphologies and similar titanium content (around 0.5% in weight), which indicates that the photocatalytic reactions did not make expressive morphologic and chemical surface changes in the TiO_2-coated PET, even after five cycles.

STEM and EELS analysis of ultra-thin cross-sections of PET-TiO_2 were also performed (Fig.3 and Fig. S1). Due to the high flexibility of the PET substrate, sample preparation was challenging and aggressive to the coated material. During TEM experiments, a heterogeneous film was visualized and EELS analysis and elementary chemical mapping was performed in that region in order to confirm if it was a part of the destroyed TiO_2 coating. Therefore, although it has been damaged, it was confirmed that the white colored region is the cross section of the TiO_2 thin film deposited onto the PET substrate (Fig. 3(a)). The obtained EELS spectrum of this region is detailed in Supplementary Material (Fig. S1 – Supplementary material) and confirms the chemical

state of the titanium detected by the chemical mapping.

Micrographs in nanometric scale are presented in Fig. 3(b), where it can be seen the coating thickness distribution (b1) and the tendency of crystallinity on the surface of the analyzed cross-section image with near-atomic resolution (b2).

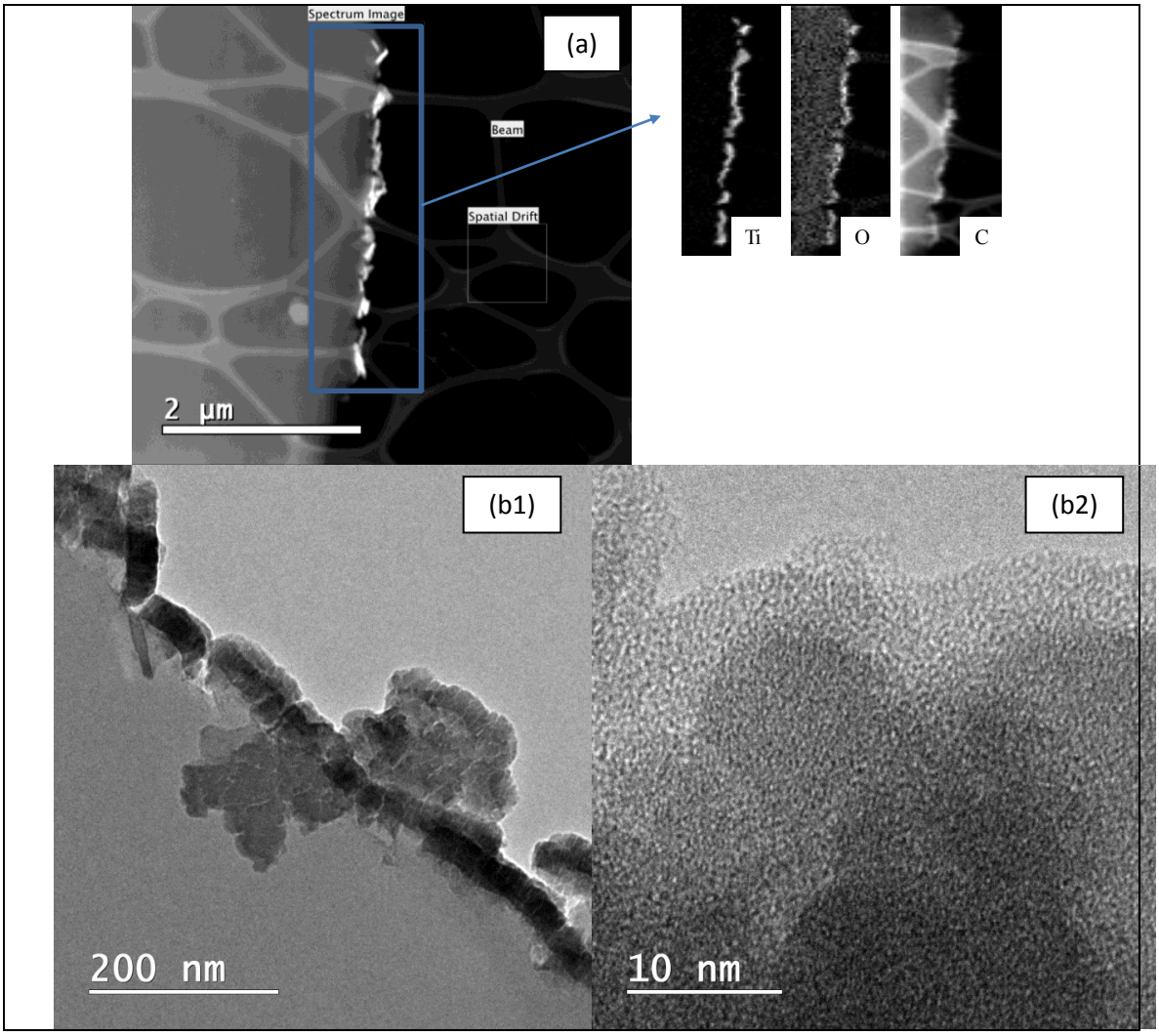

Fig. 3- (a) STEM micrographs of micrograph of the cross-sectioned PET-TiO_2 thin film with detailed titanium (Ti), oxygen (O) and carbon (C) mapping. (b1) example of heterogeneous coating thickness distribution and (b2) tendency of crystallinity on the surface of the analyzed cross-section image with near-atomic resolution.

The optical band-gap (E_g) value obtained for the PET-TiO_2, 3.25 eV (388 nm) (Fig. S2a – supplementary material), is in agreement with literature references for anatase [62,63], which gives a light adsorption edge of approximately 388 nm (UV-A irradiation). Therefore, photosensitization can be used as an alternative for improving the solar spectrum efficiency and promoting a solar photocatalytic process.

Water droplet contact angle results are presented in Fig. 4. Contact angles above 90° indicate hydrophobicity of the surface, whereas contact angles below 90º indicate hydrophilicity. The phenomenon of photoinduced hydrophilicity is frequently used as an indirect indication of self-cleaning properties and photocatalytic activity [64,65].

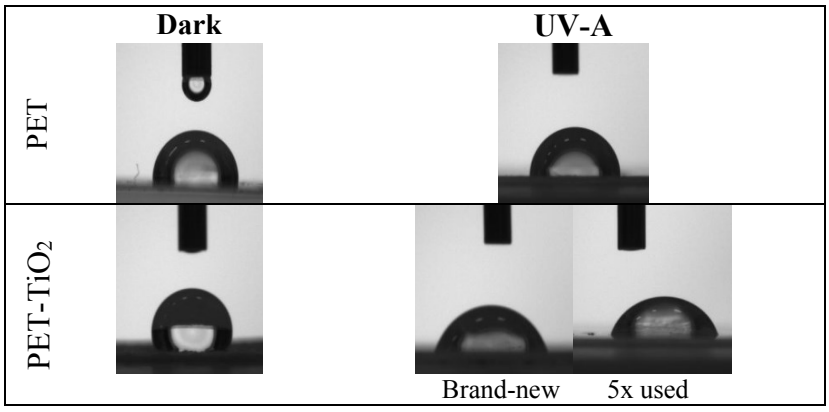

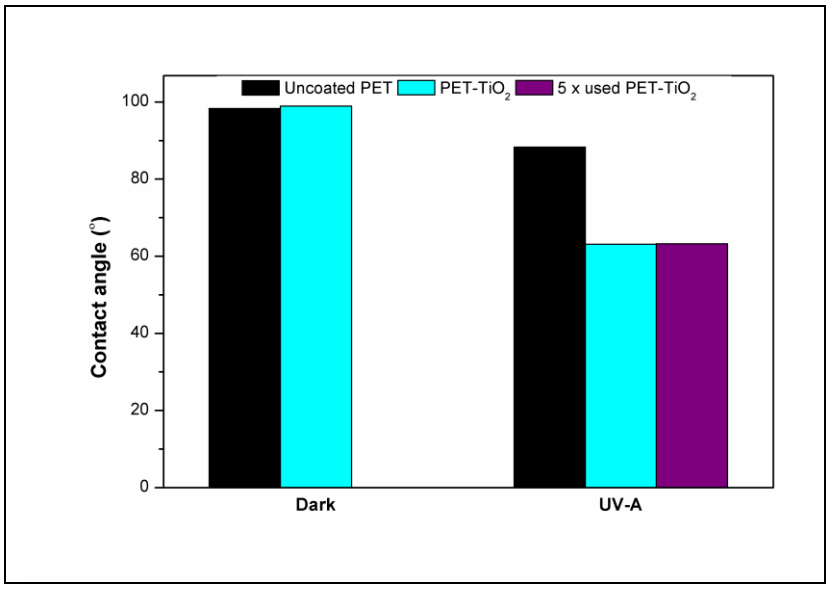

Fig. 4 - Water droplet contact angles for the uncoated PET surface (PET) and coated PET-TiO_2, comparing the brand-new surface and the surface used for 5 times.

Irradiated PET-TiO_2 presented hydrophilic behavior, while uncoated PET and PET-TiO_2 kept in the dark presented a near hydrophobic performance. These results may indicate that a photoinduced wettability phenomenon occurred and, therefore, the surface may present photocatalytic activity. In this sense, Banerjee *et al.* (2015) stated that different mechanisms have been suggested to explain the photoinduced hydrophilicity exhibited by TiO_2, including the photoinduced removal of the carbonaceous layer present on TiO_2 surfaces exposed to air (related to photocatalytic activity), the photoinduced reconstruction of surface hydroxyl groups and the generation of light-induced surface vacancies [65]. Moreover, self-cleaning properties can be interesting in real scale applications.

In addition, the contact angle of the irradiated brand new PET-TiO_2 is comparable to the contact angle of the PET-TiO_2 used 5 times. This may also indicate that the material preserved its photocatalytic activity after five cycles of use.

Selected AFM 3D topography micrographs (Fig. 5) show that the samples presented moderate to low R_{rms} roughness, with an average value of 4.48 nm for the uncoated PET, against 4.53 nm and 4.75 nm, for brand new and the 5 times used surfaces, respectively. Average surface areas had comparable values for new PET-TiO_2 surfaces and for the five times used surfaces, with variation below 1%. It can be seen, in agreement with SEM micrographs, that the new PET-TiO_2 photocatalytic surfaces presented homogeneous, smooth and dense surfaces. It can be seen that the surface of the used PET-TiO_2 is less smooth, with the presence of some scratches, but the thin film is still present, as shown in the SEM/EDS analysis.

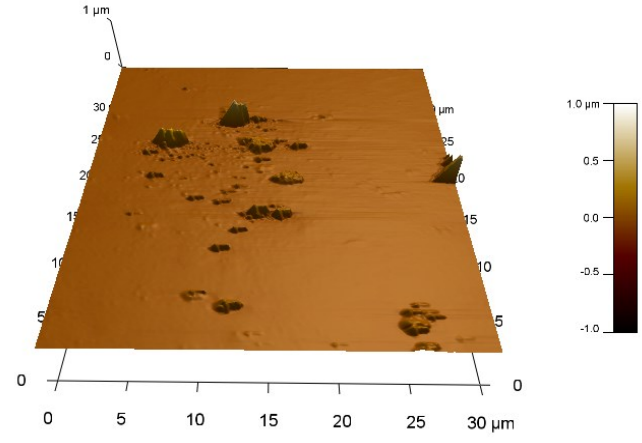

(a)

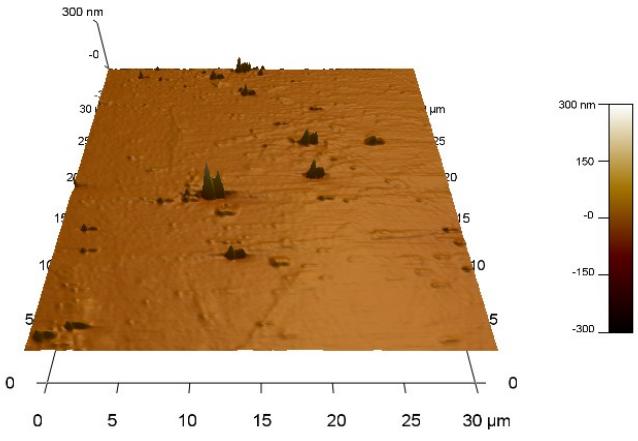

(b)

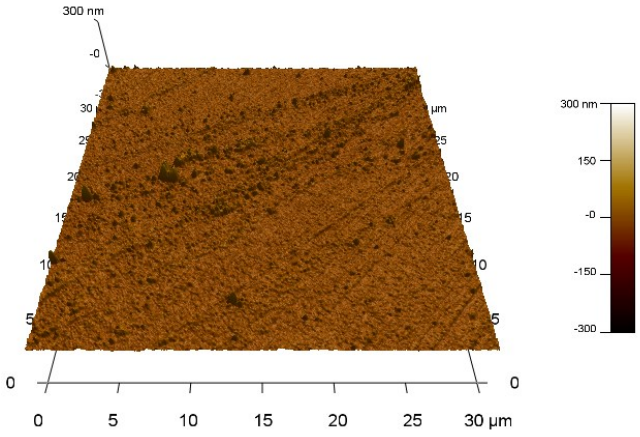

(c)

Fig. 5- Selected AFM 3D topography micrographs of 900µm^2 regions of the: (a) uncoated PET, (b) brand new PET-TiO_2 and (c) PET-TiO_2 after 5 x of use.

3.2 Photocatalytic activity results

The photocatalytic degradation of CBZ and CAF is shown in Fig. 6. Firstly, a round of experiments with CBZ (Fig. 6(a) - black squares) in the dark showed that there was no significant effect of adsorption of the CBZ molecule on the new PET-TiO_2 over 420 min. Similar results were obtained for the CAF adsorption experiments (Fig. 6(b)-black squares).

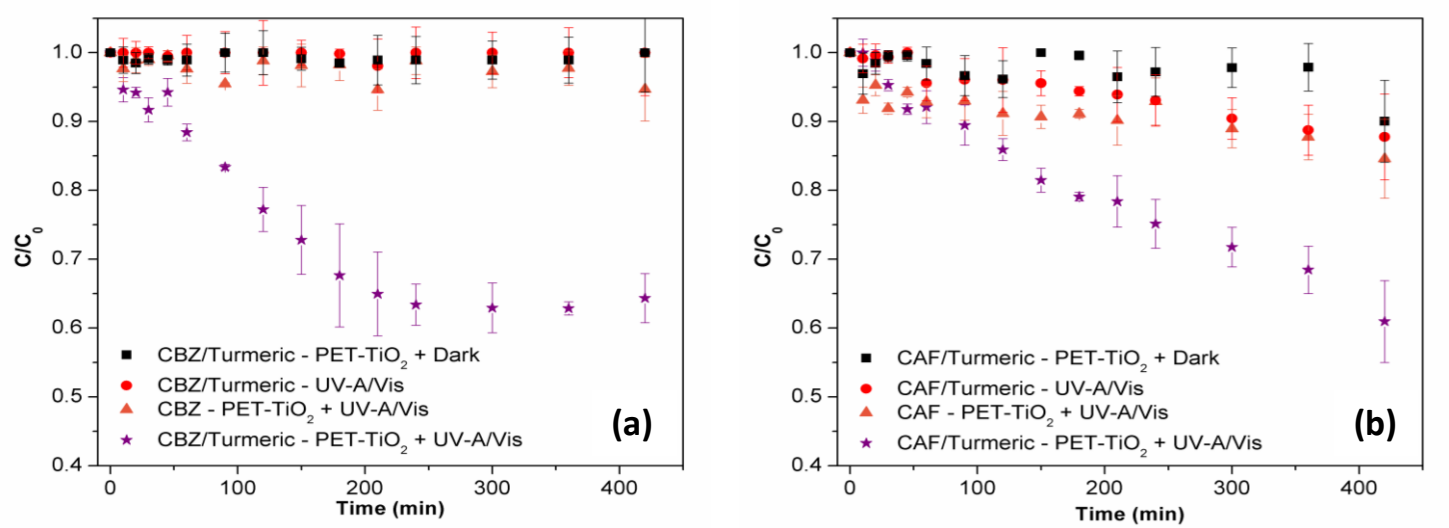

Fig. 6 - CBZ (a) and CAF (b) removal during adsorption with turmeric (PET-TiO_2 +Dark), photolysis assisted by turmeric (UV-A/Vis), photocatalysis (PET-TiO_2 + UV-A/Vis) and photocatalysis assisted by turmeric (n=3).

Photolysis control experiments under UV-A/Vis irradiation and turmeric were performed (Fig. 6 - red circles) and it can be seen that the CBZ and CAF molecules do not significantly absorb UV-A or visible radiation of wavelengths >300 nm, even in the presence of the photosensitizer (PS) turmeric. The photostability of the CBZ and CAF molecules is reported in the literature [9,47] and can also be predicted by the UV-Vis spectrophotometry scans (Figures S3 and S4 – supplementary material).

In the experiments with the PET-TiO_2 without the PS (turmeric) the results showed slower kinetics (Fig. 6- orange triangles), and the addition of a natural PS showed an increase in the degradation of the CECs model pollutants (Fig. 6- purple stars). These results showed that the PET-TiO_2 combined with the turmeric PS achieved 35%

removal of the CBZ (average pseudo-first-order rate of 0.0024 min^{-1}) and a 39% removal of CAF (average pseudo-first-order rate of 0.0026 min^{-1}).

These results are comparable to other studies applying supported TiO_2. Manassero et. al (2017) used TiO_2-coated glass rings in order to promote the photocatalytic degradation of the pharmaceutical drug clofibric acid. The authors performed the reaction for 660 min and achieved similar removals (30-40 %) of the CEC concentration in reaction times of 420 min, which implies similar kinetic rates [66]. The photocatalytic degradation of caffeine was studied using composites prepared with multi-walled carbon nanotubes and three different TiO_2 materials (suspended catalysts at $1 g \cdot L^{-1}$) and they achieved pseudo-first order kinetic rate constants which varied from $4.9 \cdot 10^{-3}$ min^{-1} (in the same order of magnitude as this work) to $123 \cdot 10^{-3}$ min^{-1} with TiO_2 P25 [55].

The PS turmeric concentration suffered a substantial decay during the experiments, with a visual and spectrophotometric removal of the colour after 2h of reaction. Fig.S5 (supplementary material) shows the turmeric concentration behaviour during photolysis and photocatalysis experiments.

Curcumin, the main yellow bioactive component of the Turmeric PS, presents an intense characteristic absorption band in the 350–480 nm wavelength region [67], improving the photons absorption and therefore enhancing the activity of the photocatalytic reactions. It is notable that there was a synergy in these photocatalytic/photosensitization methods in a non-hazardous and chemical free process. It is noteworthy that higher degradation results could have been achieved if the PS was readily soluble in water, avoiding the addition of the solvent ethanol (1% m/v),

which may act as a radical scavenger. Immobilized PS or even colored polymeric supports could be alternative solutions.

Dissolved organic carbon (DOC) results and the reusability of the PET-TiO_2 up to the 5 cycles are summarized in Fig. 7. Similarly to what was observed with the CBZ and CAF absorbance decay, it can be seen that adsorption (CBZ/CAF/Tumeric-PET-TiO_2+dark) and photolysis assisted by turmeric (CBZ/CAF/Tumeric-UVA/Vis) were not able to noticeably reduce the organic matter content (Fig.7(a)). Nevertheless, there was a significant organic matter removal by the photocatalytic process assisted by turmeric (CBZ/CAF/Tumeric-PET-TiO_2+UVA/Vis), achieving 79% of mineralization.

Moreover, in order to monitor CBZ and CAF intermediate species produced during the photocatalytic degradation process, the reactions were monitored by ESI-MS and the results are shown in Figure S6. Figure S6(a) and (d) show the ESI-(+)-MS spectra from the CBZ and CAF standard solutions, with an intense ion of m/z = 192, corresponding to protonated CBZ (Fig. S6 a) while for the CAF solution it is possible to see an intense ion of m/z = 195, corresponding to protonated caffeine and a peak at m/z =217, which correspond to Caffeine+Sodium (M+Na+ -Fig. S6 d). Figures S6 (b) and (e) show the turmeric mass spectrum in the same conditions adopted in the photocatalytic runs.

The photocatalytic degradation of CBZ in the presence of the PET-TiO_2 catalytic surface and turmeric (Fig. S6 c) resulted in a high loss of the m/z = 192 signal intensity, associated with CBZ oxidation, in agreement with the data observed by UV-Vis absorbance decay. The spectra of the oxidation products show a range of different peaks, where the peak at m/z = 160 can be attributed to the protonated molecular ion

peak ($M+H^+$) of the benzimidazole isocyanate ($M-CH_3OH$) degradation product ($C_8H_6N_3O$; Mw=159), previously reported by.

The photocatalytic degradation of CAF, on the other hand, showed a removal of the intensity of the ions at m/z = 195 and 217, corresponding to protonated CAF and CAF adducedt with sodium (Fig. S6 f) and showed a signal with m/z = 149 originated by the degradation process. The intermediate signals in the ESI-MS analysis indicate that the treatment process was carried out by an oxidation mechanism, agreeing with the UV-Vis data where adsorption process was not responsible for the total removal of the model CECs (CBZ and CAF).

The reuse cycles (Fig. 7-b) proceed with no significant loss in activity, with the reaction kinetics remaining approximately constant. The pseudo-first order rate constants for each cycle varied from 0.0020 to 0.0025 min^{-1}, respectively, with a mean rate constant of 0.0024 min^{-1} (standard deviation = 0.000207). Additionally, during 5 cycles, no loss of TiO_2 was identified by Atomic Absorption Spectrometry. All the results were below the limit of detection (LOD=0.001 ppm).

The resistance to UV degradation of the PET-TiO_2 films is also of major concern. In this work, there was no apparent UV degradation of the PET material, coated by a nanometric thin TiO_2 film (~100 nm thick). Indeed, the TiO_2 thin films might have worked as UV-protective layers, as already reported in the literature [68–70].

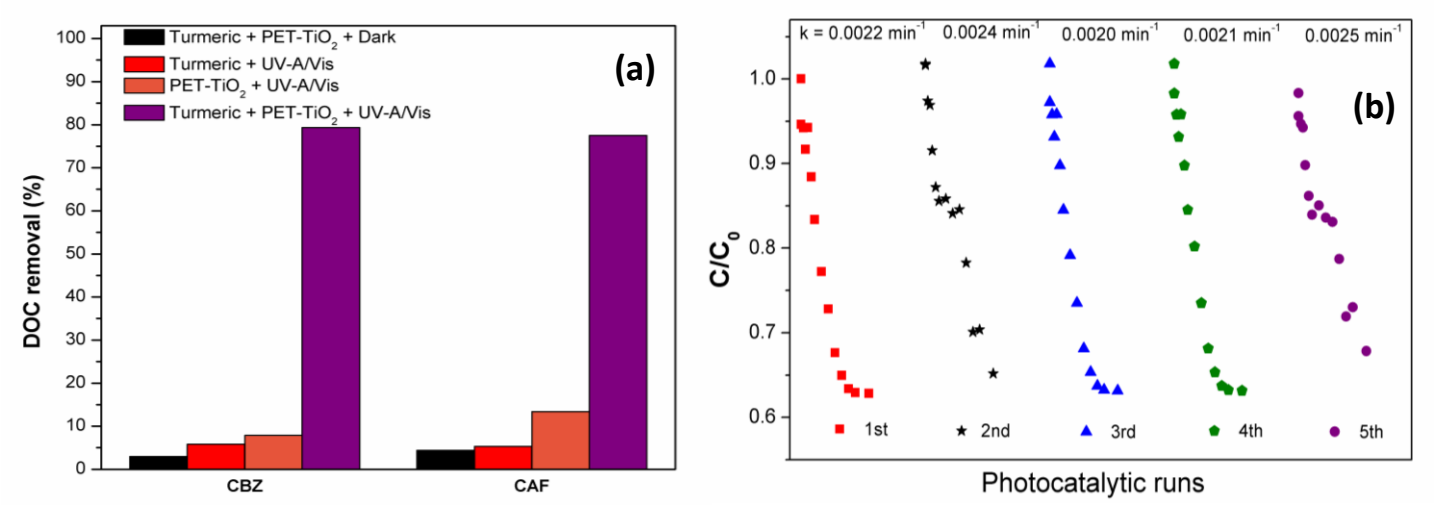

Fig. 7 – (a) Comparison of organic matter removal of the CBZ or CAF by the different processes. (b) The reusability of the PET-TiO_2: CBZ decay curves of the 5 cycles of use with detail to the pseudo-first order rate constants.

Ecotoxicity results by *Aliivibrio fischeri* showed the photocatalytic treatment assisted by turmeric PS could reduce the toxicity of the initial solution of caffeine. The CAF aqueous solution presented initial a.T.U value of 3.89 (EC_{50} = 25.69) which is considered toxic and after the photocatalytic treatment, the a.T.U. was remarkably reduced to 0.23 (EC_{50} = 433.30), which is classified as non-toxic [54,71], showing that the proposed photocatalytic treatment was able to remove the toxicity of the water solution. The ecotoxicity of the turmeric/ethanol solution (50 $mg{\cdot}L^{-1}$ and 1% ethanol) and of the ethanol solution alone (1% ethanol) were also evaluated and the results indicated that they were not toxic for the target bacteria, and the obtained values were: a.T.U = 1.15 (EC_{50} = 86.62) for the turmeric/ethanol aqueous solution and a.T.U = 0.27 (EC_{50} = 364.80) for the ethanol aqueous solution.

As for the CBZ solution, ecotoxicity results by *Aliivibrio fischeri* showed no significant changes in the CBZ solution toxicity after the photocatalytic treatment assisted by turmeric, with a slight reduction from 3.36 (EC50 = 29.76) to 3.27 (EC50 = 30.58), with the solution remaining toxic even after photocatalytic treatment.

The CBZ toxicity has been identified by other researchers as being very hard to remove. For example, da Costa et al. [72] found a similar value for a.T.U. toxicity for their non-treated CBZ water solution and the authors observed an increase of toxicity for UV photolysis and UV-H_2O_2 processes, due to the by-products formed. It can be seen in Fig.S6 that CBZ degradation by-products were obtained and one specific by-product (m/z = 160 - $M+H^+$) was identified as benzimidazole isocyanate ($C_8H_6N_3O$; Mw=159). This compound may be the one responsible for the remaining toxicity. However, in the present work, despite the fact that CBZ treated solutions retained their toxicity, we observed a slightly lower value for the photocatalytically treated solution, which means that the formation of by-products more toxic than the original pollutant did not occur.

3.3. Study of photogenerated species via trapping reactions

The results of the trapping reactions with the CAF solution with and without turmeric are shown in Fig. 8.

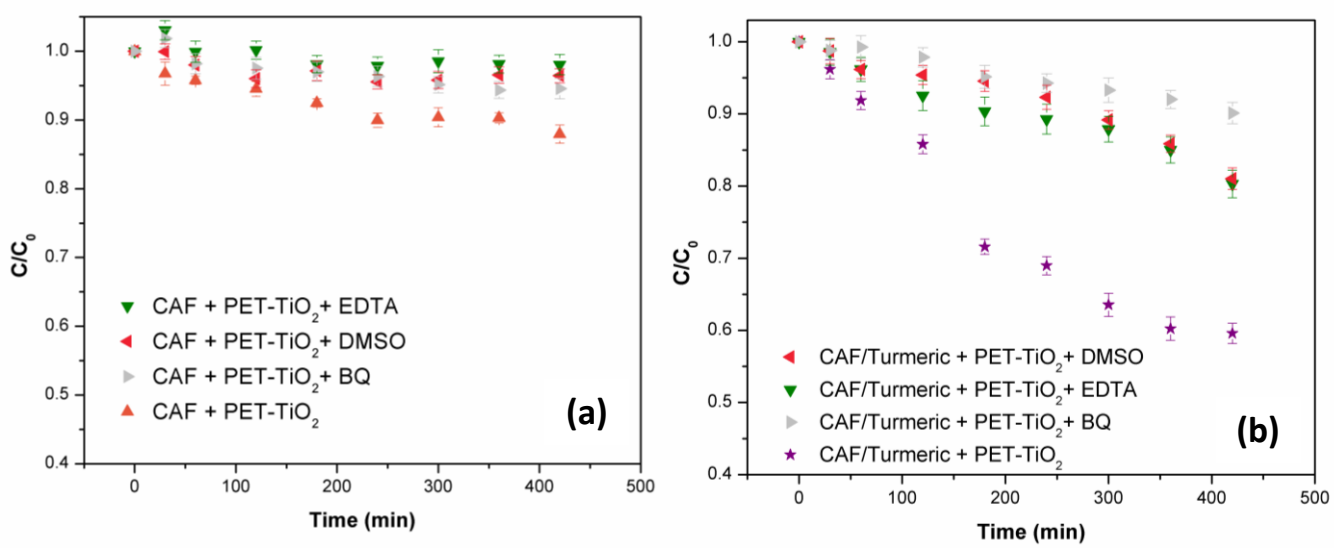

Fig. 8- CAF removal for PET-TiO_2 photocatalysis with the h^+ trapping agent (EDTA), with the $HO^\bullet$ trapping agent (DMSO) and with the $^\bullet O_2^-$ trapping agent (BQ); (a) – reactions without turmeric (b) – reactions assisted by turmeric. (n=3).

It can be seen in Fig. 8(a) that all trapping agents result in, to some extent, suppression of the degradation rate of CAF, which suggests that all 3 species ($^\bullet O_2^-$, $HO^\bullet$ and h^+) may have been generated on the photocatalytic surface, even without PS, which confirms the photocatalytic activity of the PET-TiO_2. Even though the kinetics between the different reactions presented in Fig. 8(a) are not significantly different, it seems that the h^+ scavenger EDTA (green triangle) had the most important effect and, therefore, these results suggest that the photogenerated holes (h^+) played a more important role than reactive oxygen species ($^\bullet O_2^-$ and $HO^\bullet$) .

Thus, the following simplified photoreactions might occur in the photocatalytic media [57]:

$TiO_2 \leftrightarrow h^+ + e^-$ (Eq. 2)

$O_2 + e^- \rightarrow {}^{\bullet}O_2^-$ (Eq. 3)

$OH^- + h^+ \rightarrow HO^{\bullet}$ (Eq. 4)

$H_2O + h^+ \rightarrow HO^{\bullet} + H^+$ (Eq. 5)

$CAF + h^+ \rightarrow$ OX products (Eq. 6)

$CAF + {}^{\bullet}O_2^- \rightarrow$ OX products (Eq. 7)

$CAF + HO^{\bullet} \rightarrow$ OX products (Eq. 8)

This simplified model suggests that at the beginning of the photocatalytic reactions, the photogenerated electrons and holes migrate to the surface of the catalyst (PET-TiO_2), and the electrons are captured by dissolved O_2 species to produce ${}^{\bullet}O_2^-$ radicals (Eq. 3). The generated ${}^{\bullet}O_2^-$ radicals can directly oxidize the CAF molecule (Eq. 7) simultaneously as the photogenerated holes (Eq. 6). Moreover, the h^+ can also react with H_2O and/or OH^- ions to produce $HO^{\bullet}$ (Eq. 4 and 5), which can also oxidize the CAF (Eq. 8) molecule [57].

In the presence of the turmeric PS (Fig. 8(b)), similarly to the reaction without turmeric, all types of photogenerated species may have been generated on the photocatalytic surface. It can be seen to see that the kinetics between the EDTA (green triangle) and DMSO (red triangle facing left) reactions are similar, which indicates that the effects of h^+ and $HO^{\bullet}$ are of the same significance in this photosensitized photocatalytic reaction. Fig. 8 (b-grey triangle) shows that the BQ trapping agent (${}^{\bullet}O_2^-$ scavenger) had the greatest effect on the reaction suppression and, therefore, these results suggest that in the presence of the photosensitizer the superoxide radical (${}^{\bullet}O_2^-$) played a more important

role than the other photogenerated species (h^+ and $HO^\bullet$).

Additional formation of superoxide radicals ($^\bullet O_2^-$) may be responsible for the increase in the quantum yield and photocatalytic activity of the photocatalytic process mediated by PS [73,74], which confirms the benefits of photosensitizing the reaction with non-hazardous substances. In this case, the visible-light excited photosensitizer particle promotes an electron transfer to the conduction band of the TiO_2 photocatalyst or the Ti(IV) can be converted to Ti(III) by electron capture. Also in the presence of the PS, the holes are trapped by the sensitizer, producing the corresponding excited radical [58] (Eq. 9):

$$TiO_2 + \text{Turmeric} \leftrightarrow TiO_2 (+ e^-) + \text{Turmeric}^{\bullet+} \quad \text{(Eq. 9)}$$

This electron afterwards reacts with dissolved oxygen (Eq. 3), since the reactions were performed in an open reactor vessel with low water depth and stirring, in order to guarantee consistent dissolved oxygen concentrations, promoting the formation of superoxide radicals. The photogeneration of the other species involved may still happen according to equations 4, 5, 6, 7 and 8, given earlier. Therefore, the fact that, for the photosensitizer-containing reaction, the $^\bullet O_2^-$ played the most important role in the overall photochemical process may be indicative of the synergistic effect between photocatalyst and photosensitizer.

A schematic illustration of the combination of the photosensitization and photocatalytic processes is presented in the graphical abstract. The suggested mechanism includes the photoexcitation of the turmeric photoactive compounds (PS), followed by an electron transfer to the conduction band of the photocatalyst. In the presence of solubilized oxygen, superoxide radicals may be formed and therefore, these species apparently play

an important role in the photosensitized photocatalytic process. The schematic mechanism also shows possible recombination paths and the formation of hydroxyl radicals ($HO^{\bullet}$), photogenerated holes (h^{+}) and superoxide radicals ($^{\bullet}O_2^{-}$) through the excitation of the semiconductor (photocatalysis).

These results indicate that photosensitization of TiO_2 thin films with natural turmeric showed a synergistic effect on the removal of both model pollutants (CBZ and CAF) and a mineralization of almost 80% of the initial organic matter. It has been shown that a natural non-toxic coloured compound can be utilized in order to promote photosensitization and therefore, enhance the photocatalytic degradation of CECs in a passive treatment.

Finally, the versatility of the proposed material is in the fact that photocatalytic PET surfaces could be easily scalable and utilized in different facilities present at wastewater treatment plants (WWTP), such as ponds (facultative lagoons or polishing ponds) or photo-reactors that use solar or artificial light, for CEC removal, since PET is flexible, recyclable, reusable, and easily moulded into different shaped features. Additionally, with further development, this system can take advantage of renewable solar irradiance, and of immobilized photosensitizers (such as colored PET, for example), providing a straightforward solution to the degradation of CECs from water sources, with low-cost and chemical-free reagents, as a self-cleaning, sustainable and economical process.

4. Concluding remarks

The results indicate that the PET surfaces coated with TiO_2 presented band-gap and phase characterization referent to the anatase polymorph. These results confirmed the

viability of the proposed process regarding the deposition of anatase-containing coatings directly onto flexible polymeric substrates in a single stage process without elevated process temperatures and/or post-deposition annealing requirements.

Water droplet contact angle and photocatalytic activity experiments indicated that the surfaces showed activity under UV-A radiation and it was possible to use band-gap engineering with a natural non-toxic colored compound in order to promote photosensitization and, therefore, enhance the photocatalytic degradation of recalcitrant pollutants of emerging concern in water under UV-A/Vis irradiation, reaching up to 79% of organic matter mineralization. The degradation process was also studied by ESI-MS and by-products were observed. Ecotoxicity results by *Aliivibrio fischeri* showed the photocatalytic treatment assisted by turmeric could remove the toxicity of the initial solution of caffeine and slightly reduced the initial toxicity of the carbendazim water solution, suggesting that no toxic by-products were formed.

In addition, the study of reactive oxygen species showed the prevalence of the electrogenerated hole (h^+) in the pure photocatalytic process with the PET-TiO_2 surface, while in the photosensitized process, the superoxide radical ($^{\bullet}O_2^-$) played a more important role and a possible simplified mechanism was proposed in the graphical abstract.

Finally, repeated photocatalytic experiments and characterization analysis showed that the studied photocatalytic surfaces performed with reproducible results in five cycles of utilization, which shows that the supported photocatalytic thin film can be reused in water treatment processes.

The proposed process with photocatalytic surfaces photosensitized with natural turmeric is a non-hazardous chemical-free, sustainable and straightforward potential solution for

the degradation of contaminants from water sources, and similar results were obtained for both studied recalcitrant model pollutants (CBZ and CAF).

Acknowledgement

The authors thank FAPEMIG, CAPES, CNPq and Newton Fund for their financial support, Flávia Simões for the help with the photocatalytic tests, Monique Cotrim and prof. Rodrigo Oréfice from UFMG for the photoinduced wettability tests and Ana Paula Teixeira from UFMG for the Raman spectroscopy assessment. The authors would also like to acknowledge the Center of Microscopy at the Universidade Federal de Minas Gerais (http://www.microscopia.ufmg.br) for providing the equipment and technical support for experiments involving electron microscopy.

References

[1] J.M. Herrmann, C. Duchamp, M. Karkmaz, B.T. Hoai, H. Lachheb, E. Puzenat, C. Guillard, Environmental green chemistry as defined by photocatalysis, J. Hazard. Mater. 146 (2007) 624–629. doi:http://dx.doi.org/10.1016/j.jhazmat.2007.04.095.

[2] M. Gros, K.M. Blum, H. Jernstedt, G. Renman, S. Rodríguez-Mozaz, P. Haglund, P.L. Andersson, K. Wiberg, L. Ahrens, Screening and prioritization of micropollutants in wastewaters from on-site sewage treatment facilities, J. Hazard. Mater. 328 (2017) 37–45. doi:http://dx.doi.org/10.1016/j.jhazmat.2016.12.055.

[3] M.C.V.M. Starling, C.C. Amorim, M.M.D. Leão, Occurrence, control and fate of contaminants of emerging concern in environmental compartments in Brazil, J. Hazard. Mater. (2018). doi:10.1016/j.jhazmat.2018.04.043.

[4] K. Noguera-Oviedo, D.S. Aga, Lessons learned from more than two decades of research on emerging contaminants in the environment, J. Hazard. Mater. (2016). doi:10.1016/j.jhazmat.2016.04.058.

[5] E.S. Elmolla, M. Chaudhuri, Photocatalytic degradation of amoxicillin, ampicillin and cloxacillin antibiotics in aqueous solution using UV/TiO2and UV/H2O2/TiO2photocatalysis, Desalination. (2010). doi:10.1016/j.desal.2009.11.003.

[6] A. Bernabeu, R.F. Vercher, L. Santos-Juanes, P.J. Simón, C. Lardín, M.A. Martínez, J.A. Vicente, R. González, C. Llosá, A. Arques, A.M. Amat, Solar photocatalysis as a tertiary treatment to remove emerging pollutants from wastewater treatment plant effluents, Catal. Today. 161 (2011) 235–240. doi:10.1016/j.cattod.2010.09.025.

[7] J. Carbajo, M. Jiménez, S. Miralles, S. Malato, M. Faraldos, A. Bahamonde, Study of application of titania catalysts on solar photocatalysis: Influence of type of pollutants and water matrices, Chem. Eng. J. (2016). doi:10.1016/j.cej.2016.01.092.

[8] M. Sleiman, P. Conchon, C. Ferronato, J.M. Chovelon, Iodosulfuron degradation by TiO2photocatalysis: Kinetic and reactional pathway investigations, Appl. Catal. B Environ. (2007). doi:10.1016/j.apcatb.2006.09.012.

[9] J. Saien, S. Khezrianjoo, Degradation of the fungicide carbendazim in aqueous solutions with UV/TiO2 process: Optimization, kinetics and toxicity studies, J. Hazard. Mater. 157 (2008) 269–276. doi:http://dx.doi.org/10.1016/j.jhazmat.2007.12.094.

[10] T.E. Doll, F.H. Frimmel, Kinetic study of photocatalytic degradation of carbamazepine, clofibric acid, iomeprol and iopromide assisted by different TiO2materials - Determination of intermediates and reaction pathways, Water Res. (2004). doi:10.1016/j.watres.2003.11.009.

[11] A. Manassero, M.L. Satuf, O.M. Alfano, Evaluation of UV and visible light activity of TiO2 catalysts for water remediation, Chem. Eng. J. 225 (2013) 378–386. doi:10.1016/j.cej.2013.03.097.

[12] Y. Ohko, I. Ando, C. Niwa, T. Tatsuma, T. Yamamura, T. Nakashima, Y. Kubota, A. Fujishima, Degradation of bisphenol A in water by TiO2 photocatalyst, Environ. Sci. Technol. 35 (2001) 2365–2368. doi:10.1021/es001757t.

[13] D. Nasuhoglu, D. Berk, V. Yargeau, Photocatalytic removal of 17α-ethinylestradiol (EE2) and levonorgestrel (LNG) from contraceptive pill manufacturing plant wastewater under UVC radiation, Chem. Eng. J. (2012). doi:10.1016/j.cej.2012.01.012.

[14] H.M. Coleman, K. Chiang, R. Amal, Effects of Ag and Pt on photocatalytic degradation of endocrine disrupting chemicals in water, Chem. Eng. J. (2005). doi:10.1016/j.cej.2005.07.014.

[15] F. Gonzalez-Zavala, L. Escobar-Alarcón, D.A. Solís-Casados, M. Espinosa-Pesqueira, E. Haro-Poniatowski, E. Rodríguez-Castellón, E. Rodríguez-Aguado, Synthesis and characterization of silver vanadates thin films for photocatalytic applications, Catal. Today. 305 (2018) 102–107. doi:10.1016/j.cattod.2017.09.007.

[16] M. Covei, D. Perniu, C. Bogatu, A. Duta, CZTS-TiO2thin film heterostructures for advanced photocatalytic wastewater treatment, Catal. Today. (2017). doi:10.1016/j.cattod.2017.12.003.

[17] J.C. Medina, M. Bizarro, C.L. Gomez, O. Depablos-Rivera, R. Mirabal-Rojas, B.M. Monroy, A. Fonseca-Garcia, J. Perez-Alvarez, S.E. Rodil, Sputtered bismuth oxide thin films as a potential photocatalytic material, Catal. Today. 266 (2016) 144–152. doi:10.1016/j.cattod.2015.10.025.

[18] A. Anders, Tutorial: Reactive high power impulse magnetron sputtering (R-HiPIMS), J. Appl. Phys. 121 (2017). doi:10.1063/1.4978350.

[19] S. Singh, H. Mahalingam, P.K. Singh, Polymer-supported titanium dioxide photocatalysts for environmental remediation: A review, Appl. Catal. A Gen. 462 (2013) 178–195. doi:http://dx.doi.org/10.1016/j.apcata.2013.04.039.

[20] P.J. Kelly, P.M. Barker, S. Ostovarpour, M. Ratova, G.T. West, I. Iordanova, J.W. Bradley, Deposition of photocatalytic titania coatings on polymeric substrates by HiPIMS, Vacuum. 86 (2012) 1880–1882. doi:http://dx.doi.org/10.1016/j.vacuum.2012.05.003.

[21] M. Ratova, G.T. West, P.J. Kelly, Optimisation of HiPIMS photocatalytic titania coatings for low temperature deposition, Surf. Coatings Technol. 250 (2014) 7–13. doi:10.1016/j.surfcoat.2014.02.020.

[22] M. Ratova, G.T. West, P.J. Kelly, Optimisation of HiPIMS photocatalytic titania coatings for low temperature deposition, Surf. Coatings Technol. 250 (2014) 7–13. doi:http://dx.doi.org/10.1016/j.surfcoat.2014.02.020.

[23] F. Awaja, D. Pavel, Recycling of PET, Eur. Polym. J. 41 (2005) 1453–1477. doi:10.1016/j.eurpolymj.2005.02.005.

[24] B. Geyer, G. Lorenz, A. Kandelbauer, Recycling of poly(ethylene terephthalate) – A review focusing on chemical methods, Express Polym. Lett. (2016). doi:10.3144/expresspolymlett.2016.53.

[25] V. Goudarzi, I. Shahabi-Ghahfarrokhi, A. Babaei-Ghazvini, Preparation of ecofriendly UV-protective food packaging material by starch/TiO2 bio-nanocomposite: Characterization, Int. J. Biol. Macromol. (2017). doi:10.1016/j.ijbiomac.2016.11.065.

[26] M. Abbas, H. Iftikhar, M. Malik, A. Nazir, Surface Coatings of TiO2 Nanoparticles onto the Designed Fabrics for Enhanced Self-Cleaning Properties, Coatings. 8 (2018) 35. doi:10.3390/coatings8010035.

[27] B. O'Regan, M. Grätzel, A low-cost, high-efficiency solar cell based on dye-sensitized colloidal TiO2 films, Nature. 353 (1991) 737–740. doi:10.1038/353737a0.

[28] S. Honda, H. Ohkita, H. Benten, S. Ito, Multi-colored dye sensitization of polymer/fullerene bulk heterojunction solar cells, Chem. Commun. 46 (2010) 6596. doi:10.1039/c0cc01787f.

[29] S. Venkatesan, I.-P. Liu, W.-N. Hung, H. Teng, Y.-L. Lee, Highly efficient quasi-solid-state dye-sensitized solar cells prepared by printable electrolytes for room light applications, Chem. Eng. J. 367 (2019) 17–24.

[30] S. Yano, S. Hirohara, M. Obata, Y. Hagiya, S. ichiro Ogura, A. Ikeda, H. Kataoka, M. Tanaka, T. Joh, Current states and future views in photodynamic therapy, J. Photochem. Photobiol. C Photochem. Rev. (2011). doi:10.1016/j.jphotochemrev.2011.06.001.

[31] T.G. St. Denis, T. Dai, L. Izikson, C. Astrakas, R.R. Anderson, M.R. Hamblin, G.P. Tegos, All you need is light, Virulence. (2011). doi:10.4161/viru.2.6.17889.

[32] S. Buddee, S. Wongnawa, P. Sriprang, C. Sriwong, Curcumin-sensitized TiO2 for enhanced photodegradation of dyes under visible light, J. Nanoparticle Res. 16 (2014) 2336. doi:10.1007/s11051-014-2336-z.

[33] X. Li, J.-L. Shi, H. Hao, X. Lang, Visible light-induced selective oxidation of alcohols with air by dye-sensitized TiO2 photocatalysis, Appl. Catal. B Environ. 232 (2018). doi:10.1016/j.apcatb.2018.03.043.

[34] R.B.P. Marcelino, C.C. Amorim, Towards visible-light photocatalysis for environmental applications: band-gap engineering versus photons absorption—a review, Environ. Sci. Pollut. Res. (2018). doi:10.1007/s11356-018-3117-5.

[35] S. Ghafoor, S. Ata, N. Mahmood, S.N. Arshad, Photosensitization of TiO2 nanofibers by Ag2S with the synergistic effect of excess surface Ti3+ states for enhanced photocatalytic activity under simulated sunlight, Sci. Rep. 7 (2017) 255. doi:10.1038/s41598-017-00366-7.

[36] R. Vinu, S. Polisetti, G. Madras, Dye sensitized visible light degradation of phenolic compounds, Chem. Eng. J. (2010). doi:10.1016/j.cej.2010.10.018.

[37] U. Alam, A. Khan, W. Raza, A. Khan, D. Bahnemann, M. Muneer, Highly efficient Y and V co-doped ZnO photocatalyst with enhanced dye sensitized visible light photocatalytic activity, Catal. Today. 284 (2017) 169–178.

doi:http://dx.doi.org/10.1016/j.cattod.2016.11.037.

[38] Y. Wang, J. Hong, W. Zhang, R. Xu, Carbon nitride nanosheets for photocatalytic hydrogen evolution: remarkably enhanced activity by dye sensitization, Catal. Sci. Technol. 3 (2013) 1703. doi:10.1039/c3cy20836b.

[39] F. Al-Asmari, R. Mereddy, Y. Sultanbawa, A novel photosensitization treatment for the inactivation of fungal spores and cells mediated by curcumin, J. Photochem. Photobiol. B Biol. 173 (2017) 301–306. doi:http://dx.doi.org/10.1016/j.jphotobiol.2017.06.009.

[40] Z.M. Abou-Gamra, M.A. Ahmed, Synthesis of mesoporous TiO2–curcumin nanoparticles for photocatalytic degradation of methylene blue dye, J. Photochem. Photobiol. B Biol. 160 (2016) 134–141. doi:https://doi.org/10.1016/j.jphotobiol.2016.03.054.

[41] Y. Yang, H. Wang, L. Huang, S. Zhang, Y. He, Q. Gao, Q. Ye, Effects of superabsorbent polymers on the fate of fungicidal carbendazim in soils, J. Hazard. Mater. 328 (2017) 70–79. doi:http://dx.doi.org/10.1016/j.jhazmat.2016.12.057.

[42] H. Morinaga, T. Yanase, M. Nomura, T. Okabe, K. Goto, N. Harada, H. Nawata, A Benzimidazole Fungicide, Benomyl, and Its Metabolite, Carbendazim, Induce Aromatase Activity in a Human Ovarian Granulose-Like Tumor Cell Line (KGN), Endocrinology. 145 (2004) 1860–1869. doi:10.1210/en.2003-1182.

[43] U.S.E.P.A. Office of Pesticide Programs Health Effects Division, Science Information Management Branch, "Chemicals Evaluated for Carcinogenic Potential," (2006).

[44] C.C. Montagner, C. Vidal, R.D. Acayaba, W.F. Jardim, I.C.S.F. Jardim, G. a. Umbuzeiro, Trace analysis of pesticides and an assessment of their occurrence in surface and drinking waters from the State of São Paulo (Brazil), Anal. Methods. 6 (2014) 6668. doi:10.1039/C4AY00782D.

[45] M. Loewy, V. Kirs, G. Carvajal, A. Venturino, A.M. Pechen de D'Angelo, Groundwater contamination by azinphos methyl in the Northern Patagonic Region (Argentina), Sci. Total Environ. 225 (1999) 211–218. doi:http://dx.doi.org/10.1016/S0048-9697(98)00365-9.

[46] E.S. Hsu, Central nervous system stimulants, in: Essentials Pharmacol. Anesth. Pain Med. Crit. Care, 2015: pp. 381–396. doi:10.1007/978-1-4614-8948-1_23.

[47] J.L. Rodríguez-Gil, N. Cáceres, R. Dafouz, Y. Valcárcel, Caffeine and paraxanthine in aquatic systems: Global exposure distributions and probabilistic risk assessment, Sci. Total Environ. 612 (2018) 1058–1071. doi:https://doi.org/10.1016/j.scitotenv.2017.08.066.

[48] G. Viviano, S. Valsecchi, S. Polesello, A. Capodaglio, G. Tartari, F. Salerno, Combined Use of Caffeine and Turbidity to Evaluate the Impact of CSOs on River Water Quality, Water, Air, Soil Pollut. 228 (2017) 330. doi:10.1007/s11270-017-3505-3.

[49] R. Loos, G. Locoro, S. Comero, S. Contini, D. Schwesig, F. Werres, P. Balsaa, O. Gans, S. Weiss, L. Blaha, M. Bolchi, B.M. Gawlik, Pan-European survey on the occurrence of selected polar organic persistent pollutants in ground water, Water Res. 44 (2010) 4115–4126. doi:10.1016/j.watres.2010.05.032.

[50] P. Paíga, C. Delerue-Matos, Anthropogenic contamination of Portuguese coastal waters during the bathing season: Assessment using caffeine as a chemical marker, Mar. Pollut. Bull. 120 (2017) 355–363. doi:10.1016/j.marpolbul.2017.05.030.

[51] S. Lardy-Fontan, V. Le Diouron, C. Drouin, B. Lalere, S. Vaslin-Reimann, X. Dauchy, C. Rosin, Validation of a method to monitor the occurrence of 20 relevant pharmaceuticals and personal care products in 167 bottled waters, Sci. Total Environ. 587–588 (2017) 118–127. doi:10.1016/j.scitotenv.2017.02.074.

[52] J. Tauc, R. Grigorovici, A. Vancu, Optical Properties and Electronic Structure of Amorphous Germanium, Phys. Status Solidi. 15 (1966) 627–637. doi:10.1002/pssb.19660150224.

[53] Y. Leprince-Wang, K. Yu-Zhang, Study of the growth morphology of TiO2 thin films by AFM and TEM, Surf. Coatings Technol. 140 (2001) 155–160. doi:10.1016/S0257-8972(01)01029-5.

[54] M.C.V.M. Starling, P.H.R. dos Santos, F.A.R. de Souza, S.C. Oliveira, M.M.D. Leão, C.C. Amorim, Application of solar photo-Fenton toward toxicity removal and textile wastewater reuse, Environ. Sci. Pollut. Res. 24 (2017) 12515–12528. doi:10.1007/s11356-016-7395-5.

[55] R.R.N. Marques, M.J. Sampaio, P.M. Carrapiço, C.G. Silva, S. Morales-Torres, G. Dražić, J.L. Faria, A.M.T. Silva, Photocatalytic degradation of caffeine: Developing solutions for emerging pollutants, Catal. Today. 209 (2013) 108–115. doi:10.1016/j.cattod.2012.10.008.

[56] C. Minero, G. Mariella, V. Maurino, E. Pelizzetti, Photocatalytic Transformation of Organic Compounds in the Presence of Inorganic Anions. 1. Hydroxyl-Mediated and Direct Electron-Transfer Reactions of Phenol on a Titanium Dioxide−Fluoride System, Langmuir. 16 (2000) 2632–2641. doi:10.1021/la9903301.

[57] H. Dong, G. Chen, J. Sun, C. Li, Y. Yu, D. Chen, A novel high-efficiency visible-light sensitive Ag2CO3photocatalyst with universal photodegradation performances: Simple synthesis, reaction mechanism and first-principles study,

Appl. Catal. B Environ. 134–135 (2013) 46–54. doi:10.1016/j.apcatb.2012.12.041.

[58] N.E. Polyakov, T. V Leshina, E.S. Meteleva, A. V Dushkin, T. a Konovalova, L.D. Kispert, Enhancement of the photocatalytic activity of TiO2 nanoparticles by water-soluble complexes of carotenoids., J. Phys. Chem. B. 114 (2010) 14200–4. doi:10.1021/jp908578j.

[59] S. Konstantinidis, J.P. Dauchot, M. Hecq, Titanium oxide thin films deposited by high-power impulse magnetron sputtering, Thin Solid Films. 515 (2006) 1182–1186. doi:10.1016/j.tsf.2006.07.089.

[60] K. Sarakinos, J. Alami, M. Wuttig, Process characteristics and film properties upon growth of TiOx films by high power pulsed magnetron sputtering, J. Phys. D. Appl. Phys. 40 (2007) 2108–2114. doi:10.1088/0022-3727/40/7/037.

[61] V. Tiron, I.L. Velicu, M. Dobromir, A. Demeter, F. Samoila, C. Ursu, L. Sirghi, Reactive multi-pulse HiPIMS deposition of oxygen-deficient TiOx thin films, Thin Solid Films. 603 (2016) 255–261. doi:10.1016/j.tsf.2016.02.025.

[62] W. Liu, W. Sun, A.G.L. Borthwick, T. Wang, F. Li, Y. Guan, Simultaneous removal of Cr(VI) and 4-chlorophenol through photocatalysis by a novel anatase/titanate nanosheet composite: Synergetic promotion effect and autosynchronous doping, J. Hazard. Mater. 317 (2016) 385–393. doi:http://dx.doi.org/10.1016/j.jhazmat.2016.06.002.

[63] M. Ratova, R. Marcelino, P. de Souza, C. Amorim, P. Kelly, Reactive Magnetron Sputter Deposition of Bismuth Tungstate Coatings for Water Treatment Applications under Natural Sunlight, Catalysts. 7 (2017) 283. doi:10.3390/catal7100283.

[64] J. Schneider, M. Matsuoka, M. Takeuchi, J. Zhang, Y. Horiuchi, M. Anpo, D.W. Bahnemann, Understanding TiO 2 Photocatalysis: Mechanisms and Materials, Chem. Rev. 114 (2014) 9919–9986. doi:10.1021/cr5001892.

[65] S. Banerjee, D.D. Dionysiou, S.C. Pillai, Self-cleaning applications of TiO<inf>2</inf> by photo-induced hydrophilicity and photocatalysis, Appl. Catal. B Environ. 176–177 (2015) 396–428. doi:10.1016/j.apcatb.2015.03.058.

[66] A. Manassero, M.L. Satuf, O.M. Alfano, Photocatalytic degradation of an emerging pollutant by TiO2-coated glass rings: a kinetic study, Environ. Sci. Pollut. Res. 24 (2017) 6031–6039. doi:10.1007/s11356-016-6855-2.

[67] D. Patra, C. Barakat, Synchronous fluorescence spectroscopic study of solvatochromic curcumin dye, Spectrochim. Acta Part A Mol. Biomol. Spectrosc. 79 (2011) 1034–1041. doi:https://doi.org/10.1016/j.saa.2011.04.016.

[68] J. Xu, H. Nagasawa, M. Kanezashi, T. Tsuru, UV-Protective TiO2 Thin Films with High Transparency in Visible Light Region Fabricated via Atmospheric-Pressure Plasma-Enhanced Chemical Vapor Deposition, ACS Appl. Mater. Interfaces. 10 (2018) 42657–42665. 10.1021/acsami.8b15572.

[69] M.E. El-Naggar, T.I. Shaheen, S. Zaghloul, M.H. El-Rafie, A. Hebeish, Antibacterial Activities and UV Protection of the in Situ Synthesized Titanium Oxide Nanoparticles on Cotton Fabrics, Ind. Eng. Chem. Res. (2016). doi:10.1021/acs.iecr.5b04315.

[70] F. Akhavan Sadr, M. Montazer, In situ sonosynthesis of nano TiO2on cotton fabric, Ultrason. Sonochem. (2014). doi:10.1016/j.ultsonch.2013.09.018.

[71] E.P. da Costa, S.E.C. Bottrel, M.C.V.M. Starling, M.M.D. Leão, C.C. Amorim, Degradation of carbendazim in water via photo-Fenton in Raceway Pond Reactor: assessment of acute toxicity and transformation products, Environ. Sci. Pollut. Res. (2018) 1–13. doi:10.1007/s11356-018-2130-z.

[72] E.P. da Costa, S.E.C. Bottrel, M.C.V.M. Starling, M.M.D. Leão, C.C. Amorim, Degradation of carbendazim in water via photo-Fenton in Raceway Pond Reactor: assessment of acute toxicity and transformation products, Environ. Sci. Pollut. Res. (2018). doi:10.1007/s11356-018-2130-z.

[73] V. Iliev, D. Tomova, Photocatalytic oxidation of sulfide ion catalyzed by phthalocyanine modified titania, Catal. Commun. 3 (2002) 287–292. doi:10.1016/S1566-7367(02)00122-X.

[74] X. Zhang, T. Peng, S. Song, Recent advances in dye-sensitized semiconductor systems for photocatalytic hydrogen production, J. Mater. Chem. A. 4 (2016) 2365–2402. doi:10.1039/c5ta08939e.